MARCINKOWSKI, M. J. & DAS, E. S. P. (1972). *Phil. Mag.* **26**, 1281–1300.
MARCINKOWSKI, M. J., DAS, E. S. P. & SADANANDA, K. (1973). *Phys. Stat. Sol.* (*a*) **19**, 67–81.
MARCINKOWSKI, M. J. & DWARAKADASA, E. S. (1973). *Phys. Stat. Sol.* (*a*) **19**, 597–608.
MARCINKOWSKI, M. J. & SADANANDA, K. (1973). *Phys. Stat. Sol.* (*a*) **18**, 361–375.
MARCINKOWSKI, M. J., SADANANDA, K. & TSENG, W. F. (1973). *Phys. Stat. Sol.* (*a*) **17**, 432–433.
MARCINKOWSKI, M. J. & TSENG, W. F. (1970). *Metallurg. Trans.* **1**, 3397–3401.
MARCINKOWSKI, M. J., TSENG, W. F. & DWARAKADASA, E. S. (1974). *J. Mater. Sci.* **9**, 29–40.
NABARRO, F. R. N. (1967). *Theory of Crystal Dislocations.* Oxford: Clarendon Press.
NYE, J. F. (1957). *Physical Properties of Crystals.* Oxford: Clarendon Press.
SADANANDA, K. & MARCINKOWSKI, M. J. (1973). *Scripta Met.* **7**, 557–564.
SADANANDA, K. & MARCINKOWSKI, M. J. (1974*a*). *J. Mater. Sci.* **9**, 245–257.
SADANANDA, K. & MARCINKOWSKI, M. J. (1974*b*). *J. Appl. Phys.* **45**, 1533–1543.
SADANANDA, K. & MARCINKOWSKI, M. J. (1974*c*). *J. Appl. Phys.* **45**, 1521–1532.
TSENG, W. F., MARCINKOWSKI, M. J. & DWARAKADASA, E. S. (1974). *J. Mater. Sci.* **9**, 41–56.
WIT, R. DE (1970). *Fundamental Aspects of Dislocation Theory.* NBS Special Publication No. 317, Edited by J. A. SIMMONS, R. DE WIT and BULLOUGH, Vol. 1. pp. 651–673.

Acta Cryst. (1975). A**31**, 292

Theory of Simple Two-Phase Interfaces*

BY M. J. MARCINKOWSKI,† K. SADANANDA AND W. H. CULLEN JR‡

Engineering Materials Group and Department of Mechanical Engineering, University of Maryland, College Park, Maryland 20742, *U.S.A.*

(*Received* 4 *September* 1974; *accepted* 10 *January* 1975)

The coincidence-site-lattice theory of grain boundaries has been applied to simple two-phase boundaries. Symmetric and unsymmetric tilt boundaries, pure twist boundaries and unrotated and untwisted boundaries have all been considered. It has been shown that each type of boundary can be described in terms of a characteristic coincidence-site lattice. In addition, the dislocation content within the interphase boundaries has been defined in terms of Burgers circuits described with respect to the original crystal lattices in the new coincidence-site lattices.

Introduction

It was first proposed that a coherent boundary between two phases of differing lattice constant could be described in terms of interface dislocations (Marcinkowski, 1970*a*). Those interface dislocations were originally referred to as virtual dislocations, since they appeared then to be fundamentally different from crystal-lattice dislocations. The subsequent development of the coincidence-site-lattice theory of grain boundaries however showed this not to be the case (Marcinkowski & Sadananda, 1973).

Although a number of preliminary treatments of interface dislocations have been presented (Marcinkowski, 1970*a*,*b*; Marcinkowski & Tseng, 1970; Marcinkowski, 1972; Sadananda & Marcinkowski, 1974*a*; Cullen, Marcinkowski & Das, 1973), none has yet been extensive. It is the purpose of the present effort to carry out the first of such studies. The presentation will be pedagogic in nature, relying heavily on simple geometric models. A fuller mathematical analysis will follow in a subsequent publication (Marcinkowski & Kröner, 1975). The analysis will be confined to what is perhaps the simplest of all two-phase boundaries in which the two phases A and B possess the same simple cubic structures but have differing interplanar spacings a_0 and b_0 such as shown in Fig. 1(*a*). The two-phase interface may be visualized as comprised of a parallel array of edge-type interface dislocations (shown dotted) associated with each interatomic spacing in which the Burgers vector of each interface dislocation is given by

$$|\mathbf{b}_{IB}| = a_0 - b_0. \qquad (1)$$

For the particular case shown in Fig. 1(*a*), $b_0 = \frac{9}{10}a_0$.

It is apparent that the array of interface dislocations shown in Fig. 1(*a*) generate long-range stresses In order that these stresses be reduced, an array of edge-type crystal-lattice dislocations of strength $|\mathbf{b}_{CL}| = b_0$ can be introduced into the boundary as shown by the solid dislocation symbols in Fig. 1(*b*). It is a simple matter to show that the long-range stresses are fully compensated when the spacing between the crystal-

* The present research effort was supported by The National Science Foundation under Grant No. GH-32262.

† Presently on sabbatical leave at Institut für Theoretische und Angewandte Physik der Universität Stuttgart, Germany (BRD).

‡ Now with the U. S. Naval Research Laboratory, Washington, D. C. 20390.

lattice dislocations R is given by (Cullen, Marcinkowski & Das, 1973)

$$R = na_0 \qquad (2a)$$

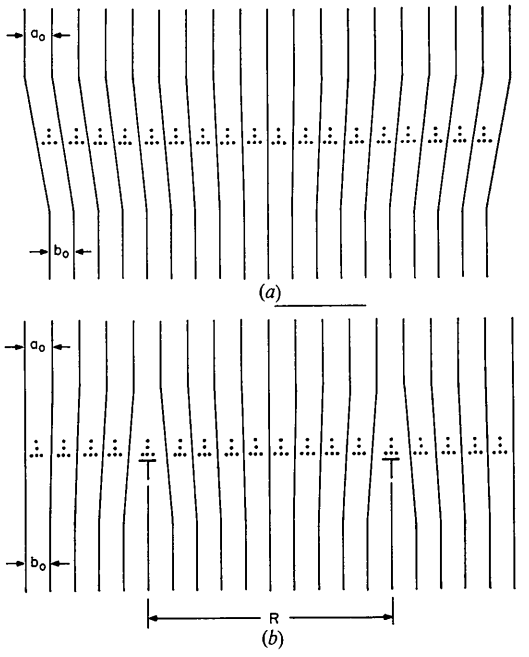

Fig. 1. (*a*) Simple boundary between two coherent phases described in terms of interface dislocations. (*b*) Same boundary as in (*a*) but which now contains misfit dislocations.

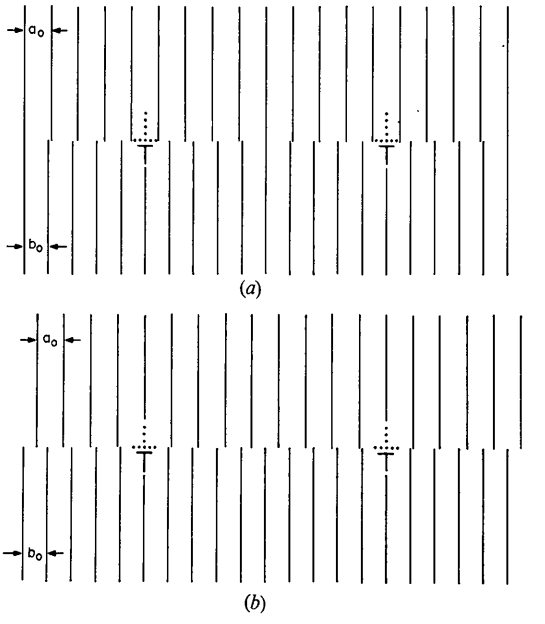

Fig. 2. Same interphase boundary as that shown in Fig. 1(*b*) but with the interphase dislocations now coalesced on the crystal-lattice dislocations. (*a*) Case where coalesence occurs equally from both sides of crystal-lattice dislocation. (*b*) Case where coalesence occurs entirely from the left of each crystal-lattice dislocation.

where n is the number of interatomic spacings measured in terms of lattice A or by

$$R = Nb_0 \qquad (2b)$$

where

$$N = n+1\,, \qquad (2c)$$

where N is the number of interatomic spacings measured in terms of lattice B. In the specific case of Fig. 1(*b*), $n=9$.

As the following sections will show, interface dislocations play the same role in two-phase interfaces as grain boundary dislocations (GBD) play in grain boundaries. For this reason therefore interface dislocations will henceforth be termed interphase boundary dislocations (IBD), while the misfit dislocations, which play the role of crystal lattice dislocations (CLD) in grain boundaries, will also be termed (CLD) in the case of two phase interfaces.

Configuration of interphase boundary dislocations within the interface

For simplicity, Fig. 1(*b*) shows the IBD to be arranged uniformly. In reality however this uniform array is expected to be significantly perturbed by the CLD which possess much larger Burgers vectors than the IBD. More specifically, the IBD are expected to be drawn towards the CLD, and in fact undergo mutual annihilation. The results of this annihilation are shown by the interface configurations of Figs. 2(*a*) and 2(*b*). In the case of Fig. 2(*a*), the IBD are drawn equally from both sides of each CLD, *i.e.* four from each side, while in the case of Fig. 2(*b*), all eight IBD lying toward the left of each CLD are drawn coincidentally toward each CLD. Except for the small ledges formed at both surfaces of Fig. 2(*b*), the interphase configurations in Figs. 2(*a*) and 2(*b*) are identical. It is apparent that each of the IBD shown in these two figures now have Burgers vectors given by

$$n\mathbf{b}_{IB} = 9\mathbf{b}_{IB} = -\mathbf{b}_{CL}\,. \qquad (3)$$

Note that since there is complete annihilation between all of the IBD and CLD in Figs. 2(*a*) and 2(*b*), no elastic distortions remain at the interface. On the other hand, the corresponding planes in phases A and B are no longer continuous across the interface, but instead are offset from one another. These offsets may be considered analogous to stacking faults in a single phase, with the exception that the fault energy is now a function of position along the fault plane since the magnitude of the offsets varies along the interphase boundary.

It is a simple matter to speculate on the role of the faults in the interphase boundary of Fig. 2. In particular, they will act to resist the motion of the IBD, shown in Fig. 1, to the CLD. The net result will be a IBD–CLD configuration intermediate between that

depicted in Figs. 1 and 2 depending upon the stacking-fault energy. As is usually the case, it is extremely difficult to calculate the stacking-fault energies associated with the interfaces of Fig. 2, since such calculations depend upon the nature of the bonding across the interface. In general however it is expected that the IBD will be clustered about the CLD, the cluster becoming tighter as the stacking-fault energy decreases.

It might be expected that in the case where the elastic constants between the two phases are different from one another that the effective Burgers vectors of the IBD and CLD would be altered. Such is indeed the case, and such alteration requires the superposition of image forces (Hirth & Lothe, 1968; Weertman & Weertman, 1964). However since both types of dislocations lie entirely within the interface, their Burgers vectors are altered by the same factor, so that equation (3) still obtains. The relationship between the number of IBD and CLD required for complete interphase boundary compensation is thus seen to be a geometric property, independent of the particular physical properties of the crystal.

Coincidence-site-lattice representation of an interphase boundary

The interphase boundaries discussed thus far can also be represented in terms of the coincidence-site-lattice model which has been of great success in describing grain boundaries (Marcinkowski & Sadananda, 1973; Marcinkowski, Sadananda & Tseng, 1973; Sadananda & Marcinkowski, 1974*b*). This is most conveniently done by referring to the vertical interphase boundary in Fig. 3 in which $b_0=\frac{4}{5}a_0$. The boundary is seen to be fully compensated and stress free similar to that shown in Fig. 2(*a*). The open circles correspond to coincidence sites within the boundary, *i.e.* points at which atom sites in phases *A* and *B* coincide.

It is now possible to construct unit cells associated with the interphase boundary of Fig. 3 as illustrated in Fig. 4. One unit cell is drawn with respect to the *A* phase and another with respect to the *B* phase with the boundary separating the two. It is apparent that both unit cells are of identical edge length a_{0c} given by

$$a_{0c}=R=na_0=Nb_c \qquad (4)$$

and will be termed coincidence-site-lattice unit cells. The values of N and n are related by equation 2(*c*). It is also to be noted that each of the coincidence-site-lattice unit cells can be subdivided into sublattices in the manner shown by the dashed lines in Fig. 4. For clarity, the dashed lines are drawn in only one direction within the top and bottom portions of the coincidence-site-lattice unit cells. Each sublattice unit cell has an edge length given by a_{0cs} where it is apparent that

$$a_{0cs}=\frac{a_0}{N}=\frac{b_0}{n}. \qquad (5)$$

In the case of Fig. 4, $n=4$ and $N=5$. Equations (1), (2*c*) and (5) when combined give

$$|\mathbf{b}_{IB}|=a_{0cs}. \qquad (6)$$

The physical meaning of the IPB dislocation now becomes clear in terms of the quantity a_{0cs} in equation (6) when it is realized that a coherent interphase boundary of the type shown in Fig. 1(*a*) may be viewed in terms of an extra half plane of magnitude a_{0cs} spaced uniformly within each crystal-lattice unit cell of the *A* phase. One such extra half plane is shown within a crystal lattice unit cell by the shaded area in Fig. 5 based upon the interphase boundary shown in Fig. 4.

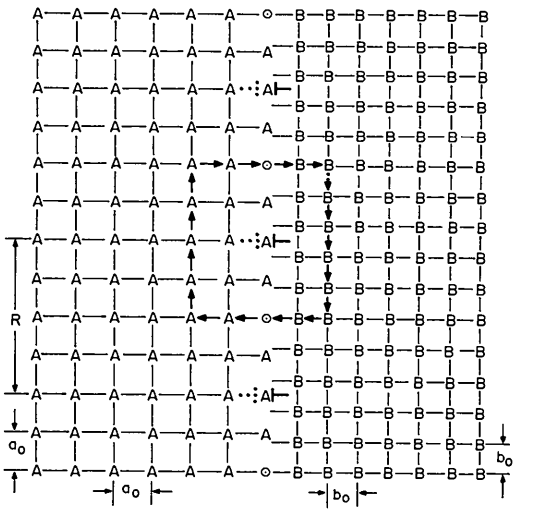

Fig. 3. Fully stress-free interphase boundary.

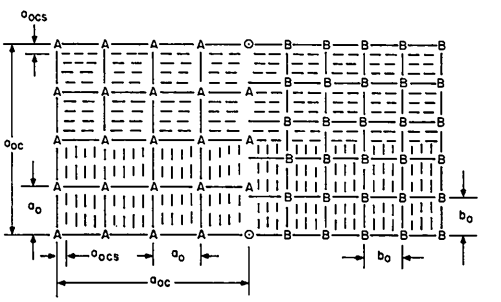

Fig. 4. Pair of coincidence-site-lattice unit cells associated with the interphase boundary shown in Fig. 3.

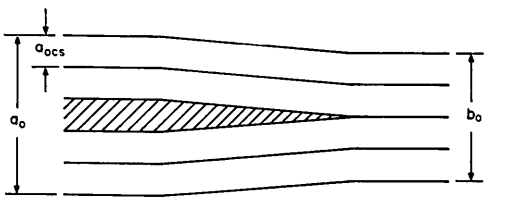

Fig. 5. Interpretation of the interphase boundary dislocation in terms of the coincidence-site-lattice sublattice.

Interphase tilt boundaries

As for the case of a grain boundary in a single-phase material, it is possible to construct a symmetric tilt boundary between two different phases. In particular,

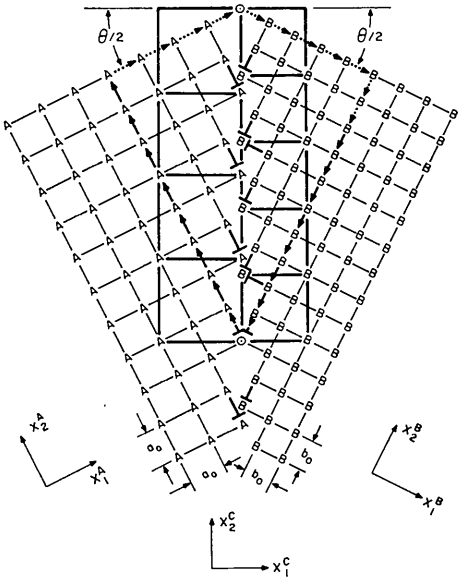

Fig. 6. A 53·1° symmetric interphase tilt boundary.

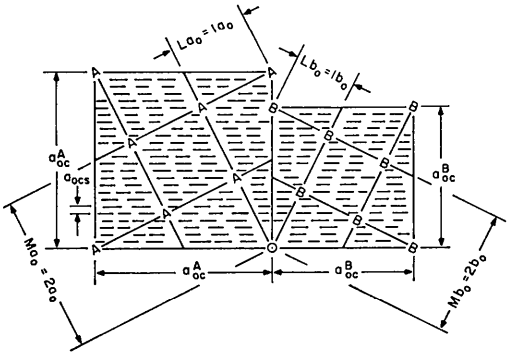

Fig. 7. Further subdivision of the coincidence-site-lattice unit cell associated with the symmetric interphase boundary of Fig. 6 into a smaller sublattice.

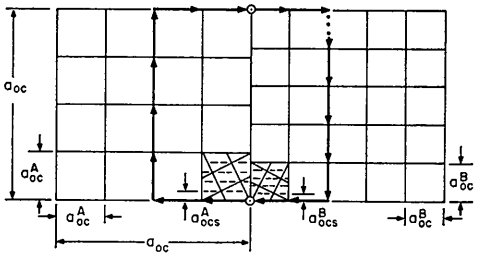

Fig. 8. Pair of coincidence-site-lattice unit cells associated with the 53·1° symmetric interphase boundary shown in Fig. 6.

consider the counterclockwise and clockwise rotations of phases A and B respectively shown in Fig. 3 by $\theta/2$ with respect to the vertical interphase boundary. If θ is chosen as 53·1°, the symmetric tilt boundary of Fig. 6 obtains. It will be noted that each phase possesses its own characteristic coincidence-site lattice (Marcinkowski, Sadananda & Tseng, 1973; Marcinkowski & Sadananda, 1975) which can be characterized by the following coincidence-site-lattice relationships. For phase A

$$\tan\theta/2=\frac{La_0}{a_0}=\frac{L}{M} \qquad (7a)$$

while for phase B

$$\tan\theta/2=\frac{Lb_0}{Mb_0}=\frac{L}{M}\,. \qquad (7b)$$

The meanings of L and M can be discerned from inspection of Fig. 7 where it can be seen that they may be thought of as the number of dislocations of strength a_0 or b_0 which have moved into the boundary over glide planes with normals X_2^A or X_2^B respectively, separated M atom spacings apart. The position of each one of these dislocations in Fig. 6 is seen to simply represent the terminus of an extra half plane with normal X_1^A or X_1^B within either phase A or B respectively. For the particular case of Figs. 6 and 7, $L=1$ while $M=2$, from which equations (7) both give $\theta=53{\cdot}1°$.

It is clear from Figs. 6 and 7 that the coincidence-site lattices for each grain are of different size, *i.e.*, a^A_{oc} for phase A and a^B_{oc} for phase $1B$, and thus do not by themselves correspond to the coincidence-site lattice common to the entire grain boundary. It can be seen however from Fig. 6 that such a common coincidence-site lattice can be obtained by combining four coincidence-site lattices associated with phase A with five coincidence-site lattices associated with phase B along the two-phase boundary. A more complete representation of a pair of such coincidence-site-lattice unit cells of edge length a_{0c} can be seen in Fig. 8. Comparison of Figs. 6 and 8 with Figs. 3 and 4 respectively show that a^A_{oc} and a^B_{oc} for a symmetric tilt-type two-phase boundary play the same role as a_0 and b_0 for a corresponding two-phase boundary in which $\theta=0$. Thus it is possible to use n and N given by equation (2c) for the relative number of a^A_{oc} and a^B_{oc} type unit cells lying along the symmetric tilt boundary. Furthermore, in analogy with equation (4)

$$a_{0c}=na^A_{oc}=Na^B_{oc}\,. \qquad (8)$$

The dislocations which compensate the misfit parallel to the interphase boundary due to the differences in a^A_{oc} and a^B_{oc} are shown by the CLD in Fig. 6 which lie within phase B and which are the termini for the extra half planes whose normals are along X_2^B. More will be said about these particular dislocations when the question of the Burgers circuit is taken up in a subsequent section.

Fig. 8 shows that the coincidence-site lattices with unit-cell edges a^A_{oc} and a^B_{oc} can be further subdivided into sublattices with unit cells a^A_{ocs} and a^B_{ocs} respectively. For clarity, the subdivision has been shown only in terms of a horizontal set of dashed lines. The vertical lines, which would have completed the subdivision, have been omitted. It has already been shown (Marcinkowski & Sadananda, 1975) that

$$a^A_{ocs} = \frac{a^A_{oc}}{(L^2+M^2)} \tag{9a}$$

while

$$a^B_{ocs} = \frac{a^B_{oc}}{(L^2+M^2)} . \tag{9b}$$

Fig. 7 also shows that a_0 associated with the entire two-phase symmetric tilt boundary in Fig. 6 can also be subdivided into a distinct sublattice (dashed lines) of unit-cell edge given by a_{ocs}. From this figure it is apparent that

$$a_{0cs} = a^A_{ocs} - a^B_{ocs} \tag{10a}$$

which when combined with equation (9) gives

$$a_{0cs} = \frac{a^A_{oc}(N-n)}{N(L^2+M^2)} . \tag{10b}$$

Upon substitution of the integers appropriate to Fig. 7, *i.e.* $N=5$, $n=4$, $L=1$ and $M=2$, it is found that $a_{0cs}=a^A_{oc}/25$, in precise agreement with the construction in Fig. 7.

It is now possible to employ the coincidence-site-lattice unit cells a_{0c} associated with the two-phase tilt boundary of Fig. 6 to construct a stepped asymmetric tilt boundary of any angle in which each stepped segment consists of an identical symmetric boundary (Marcinkowski & Sadananda, 1973, 1975). The straight counterparts of these asymmetric boundaries can also be readily constructed and will be considered in more detail in the following section.

The symmetric two-phase tilt boundary illustrated in Fig. 6 is surprisingly similar to the asymmetric grain boundary associated with a single-phase material (Marcinkowski & Sadananda, 1973; Marcinkowski, Sadananda & Tseng, 1973). One such boundary is shown in Fig. 9 for $\theta = 53{\cdot}1°$. It is apparent that a characteristic coincidence-site lattice with edge length a^1_{oc} could be associated with grains #1 and #2. However it is also possible to choose a^1_{oc} as the unit cell length in grain #1 and $a^2_{oc}=a_0$ as the coincidence-site-lattice unit cell in grain #2. Clearly $a^1_{oc}=5a^2_{oc}$, and thus we have a situation resembling that given by Fig. 6 in which two types of coincidence-site-lattice unit cell may be associated with the boundary. This similarity will take on still greater significance when the Burgers circuit associated with a two-phase boundary is considered later on.

In the application of the present coincidence-site-lattice theory to grain boundaries, it was shown that the grain boundary could be visualized in terms of grain-boundary dislocations comprised of various combinations of CLD from the two adjacent grains (Marcinkowski, Sadananda & Tseng, 1973). Likewise, in the present analysis of two-phase interfaces, it seems reasonable to extend this argument. In particular, equation (1) could be written for a more general IBD as

$$\mathbf{b}_{IB} = \mathbf{b}^A_{CL} \pm \mathbf{b}^B_{CL} \tag{11}$$

where $\mathbf{b}^A_{CL}$ and $\mathbf{b}^B_{CL}$ are the Burgers vectors associated with the CLD of phases A and B respectively and which have magnitudes given by a_0 and b_0 respectively.

Before continuing further with equation (11), it is important to distinguish between two distinct types of IBD, which will be termed compensated and uncompensated respectively. Such designations were originally carried out for grain-boundary dislocations (Marcinkowski & Sadananda, 1973). The IBD of Fig. 1 correspond to uncompensated dislocations of strength

$$\mathbf{b}_{IB} = \mathbf{b}^A_{CL} - \mathbf{b}^B_{CL} = [hkl]a_{0cs} = [100]a_{0cs} \tag{12}$$

where h,k,l are integers corresponding to the number of coincidence-site-sublattice unit cells measured along the X^C_1, X^C_2 and X^C_3 axis common to the coincidence-site lattices as shown in Fig. 6. In Fig. 2(*a*), nine $\mathbf{b}_{IB}$ of strength given by equation (12) coalesce and become fully compensated by a CLD of strength $[\bar{1}00]b_0$. In a similar manner the uncompensated IBD corresponding to Fig. 5 may be written as $\mathbf{b}_{IB}=[010]a_{0cs}$. Five of these combine with a CLD of strength $[0\bar{1}0]b_0$ to produce the compensated interphase boundary of Fig. 3. Likewise if a pair of dislocations residing at each coincidence site within the interphase boundary of Fig. 6 were removed, there would remain an uncompensated IBD given by

$$\mathbf{b}_{IB} = \mathbf{b}^A_{CL} + \mathbf{b}^B_{CL} \tag{13}$$

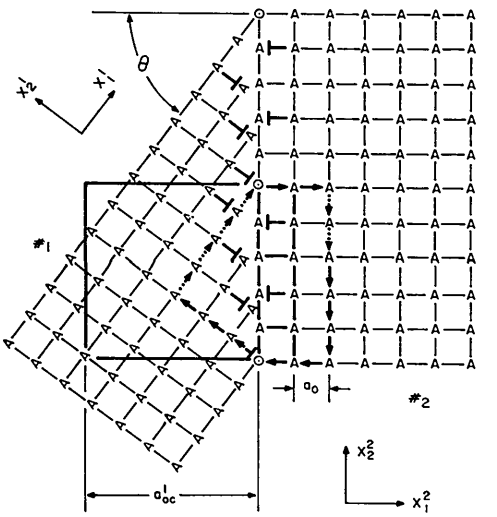

Fig. 9. A 53·1° asymmetric tilt boundary in a single-phase material.

which, with respect to the common c coordinate system, has x and y, *i.e.* 1 and 2 components, given by

$$b^1_{IB} = L(a_0 + b_0)\cos\theta/2 \qquad (14a)$$

and

$$b^2_{IB} = L(a_0 - b_0)\sin\theta/2\,. \qquad (14b)$$

From inspection of Fig. 7, equation (14) can be written as

$$b^1_{IB} = \frac{L_M(a^A_{oc} + a^B_{oc})}{(L^2 + M^2)} \qquad (15a)$$

and

$$b^2_{IB} = \frac{L^2(a^A_{oc} - a^B_{oc})}{(L^2 + M^2)} \qquad (15b)$$

which with the aid of equations (8), (9) and (10) give

$$b^1_{IB} = \frac{LM(N+n)}{(N-n)}\,a_{0cs} \qquad (16a)$$

and

$$b^2_{IB} = \frac{L^2(N-n)}{(N-b)}\,a_{0cs}\,. \qquad (16b)$$

For the coincidence sites associated with the interphase boundary of Fig. 6 equation (16) becomes $b^1_{IB} = 18a_{0cs}$ and $b^2_{IB} = 1a_{0cs}$ or more concisely

$$\mathbf{b}_{IB} = \mathbf{b}^A_{CL} + \mathbf{b}^B_{CL} = [18, 1, 0]a_{0cs}\,. \qquad (17)$$

With the exception of Fig. 1(*a*), all of the interphase boundaries discussed thus far are fully compensated. Strictly speaking, fully compensated boundaries should be illustrated by combinations of dotted and solid dislocation symbols whose total Burgers vector is zero. For convenience however, all compensated interphase boundaries will be described only in terms of the solid symbol, whereas when they become uncompensated, the dotted symbol will be employed. It has also been shown that a fully compensated grain boundary is one in which the incompatability tensor **H** associated with it vanishes (Marcinkowski & Sadananda, 1975). The same reasoning seems also appropriate for a fully compensated interphase boundary.

It will also be noted that $\mathbf{b}_{IB}$, as shown in equations (12) and (17), as well as any individual CLD lying within the interphase boundary, can always be represented in terms of a_{0cs}, the unit-cell edge associated with the complete coincidence-site lattice of the symmetric interphase tilt boundary. In this respect it is also important to note that interphase-boundary deformation associated with the passage of a dislocation from phase A to phase B in Fig. 6 may be written as (Sadananda & Marcinkowski, 1974*a*)

$$\mathbf{b}_{IB} = \mathbf{b}^A_{CL} - \mathbf{b}^B_{CL} = [210]a_{0cs}\,. \qquad (18)$$

Unlike the case of a single-phase material in which $|\mathbf{b}^A_{CL}| = |\mathbf{b}^B_{CL}|$ where the Burgers vector lies entirely within the grain boundary and is thus glissile, $\mathbf{b}_{IB}$ given by equation (18) does not give rise to a glissile IBD. In addition, $\mathbf{b}_{IB}$ in equation (18) is obviously uncompensated.

Burgers circuit associated with an interphase boundary

It has already been shown that the Burgers circuit associated with a grain boundary in a single-phase material could be described as shown by the circuit of arrows in Fig. 9, each of magnitude a_0 (Marcinkowski & Sadananda, 1973, 1975). The circuit is begun and ended on a coincidence site within the boundary by moving an equal number of steps, *i.e.* three in the case of Fig. 9 along equivalent directions in grains #1 and #2, *i.e.* X^1_2 and X^2_2. Note that the steps along X^2_1 in grain #2 just cancel one another. The closure failure is denoted by the number of excess steps and is shown by dotted arrows, *i.e.* four along X^1_1 in grain #1 and two along X^2_2 in grain #2. In a similar manner, Burgers circuits can be constructed about the interphase boundaries illustrated in Figs. 3 and 6 where again the closure failure is represented by the dotted arrows which are seen to be directly related to the number, magnitude and direction of the Burgers vectors associated with the CLD within the boundary, *e.g.* in the case of Fig. 6, four dislocations along X^A_1, five along X^B_1 and two along X^B_2.

The Burgers circuit associated with the interphase boundary of Fig. 6 could also be described in terms of the individual coincidence-site lattices a^A_{oc} and a^B_{oc} corresponding to each of the two phases as shown in Fig. 8. In this particular case, its closure failure is seen to be one Burgers vector of strength a_{0c} along X^C_2. Thus, the Burgers circuit of Fig. 8 is qualitatively the same as that given in Fig. 3 and serves only to describe the misfit parallel to the symmetric interphase tilt boundary. The tilt misfit θ is not detected in the Burgers circuit of Fig. 8. It is also apparent that the Burgers circuit could also be described with respect to the sublattice unit cells of edge length a_{0cs} in Figs. 4 and 7, however, it is obvious that the closure failure is always zero for fully compensated interphase boundaries of the type illustrated in these particular figures. Such however is not the case for the uncompensated interphase boundary such as illustrated in Fig. 1(*a*) where the closure failure is some multiple number of a_{0cs} units measured along X^C_1. Similar arguments have also been used for compensated and uncompensated grain boundaries in single-phase materials (Marcinkowski & Sadananda, 1973).

The final item of interest in this section is the two-phase counterpart of the asymmetric tilt boundary shown in Fig. 9. Such a boundary derived from Fig. 6 is shown in Fig. 10. In particular, the boundary in Fig. 10 may be derived from that in Fig. 6 by rotating the latter boundary counterclockwise by $\theta/2 = 53{\cdot}1°/2$ so that it now coincides with the X^A_2 direction of phase A.

This operation thus makes θ in Fig. 10 equal to 36·9°. A Burgers circuit taken within such a boundary, similar to that described with respect to Fig. 9, shows immediately that no closure failure exists parallel to the interphase boundary. Physically this means that the two phases exactly compensate one another in this particular orientation so that no misfit dislocations need be inserted into phase *A*. The only misfit dislocations required are those that give rise to the tilt of phase *B* with respect to phase *A* and these are all contained in phase *B*, as can be discerned from Fig. 10. Also of importance to note is the fact that the coincidence-site-lattice unit cell associated with the 36·9° asymmetric tilt boundary is smaller than that associated with the 53·1° symmetric boundary and is due to the better fit between the two phases in the former case.

Interphase twist boundaries

Fig. 11 illustrates a pure twist boundary between two different phases *A* and *B* which is bounded by two symmetric tilt boundaries. The tilt boundary toward the right is clearly of the same kind as that shown in Fig. 6. A partial reproduction of Fig. 11 is shown in Fig. 12(*a*) in which the edge dislocations which comprise the tilt portions of the interphase boundary are joined by their corresponding screw segments which are shown as straight lines. Strictly speaking, the screw segments associated with phase *B* are not of pure screw type, since the corresponding edge dislocations upon which they terminate do not lie on the same crystallographic plane, but on adjacent planes separated by a distance b_0. The reason for this is due to the insertion of additional dislocations required to accomodate the component of misfit parallel to the tilt boundaries.

It is conceivable that, as in the case of pure twist boundaries (Marcinkowski & Dwarakadasa, 1973), some of the screw-type crystal-lattice dislocations could react with each other in pairs at their coincidence-site lattice points, in accordance with a reaction of the type given by equation (13), to generate the two distinct orthogonal IBD configurations shown in Figs. 12(*b*) and 12(*c*). In the case of Fig. 12(*b*), the IBD outline a unit cell of edge length a_{0c} as described in Fig. 8, whereas in Fig. 12(*c*), the unit-cell size is much smaller and is in fact identical to that associated with the two-phase asymmetric tilt boundary shown in Fig. 10. In both cases however the Burgers vectors of the IBD are identical and are given by equation (17). Since $\mathbf{b}_{IB}$ is parallel to neither of the coincidence-site-lattice unit-cell edges associated with Figs. 12(*b*) and 12(*c*), [although this is almost the case in Fig. 12(*b*)] the dislocations are of mixed type, *i.e.* part screw and part edge. The edge segments produce no long-range stresses but in part compensate for the misfit between phases *A* and *B* across the twist boundary. Furthermore, the IBD of Figs. 12(*b*) and 12(*c*) account for only a portion of the grain-boundary structure since there are still unreacted CLD (not shown) within the interface.

Whether one sees the grain-boundary structures shown by Figs. 12(*a*), 12(*b*), 12(*c*) or combinations thereof, say when viewed within the electron microscope by transmission techniques, depends upon the nature of the contrast being employed (Marcinkowski, Tseng & Dwarakadasa, 1974*a*). If strain contrast is utilized, the particular structure observed will depend upon the degree of relaxation associated with each particular configuration, which in turn will depend upon the most stable energy configuration associated with that given dislocation configuration (Sadananda & Marcinkowski, 1974*b*). In this respect, it has been argued that those coincidence-site-lattice unit cells which are small will be energetically favorable (Bollmann, 1970). This would mean that the dislocation configuration shown in Fig. 12(*c*) would be favored over that in Fig. 12(*b*), while the asymmetric tilt boundary of Fig. 10 would be favored over the corresponding symmetric one depicted in Fig. 6.

In concluding the present study a number of general comments can be made. In the first place, all of the two-phase boundaries discussed in the previous sections possessed rotation axes which were parallel to the

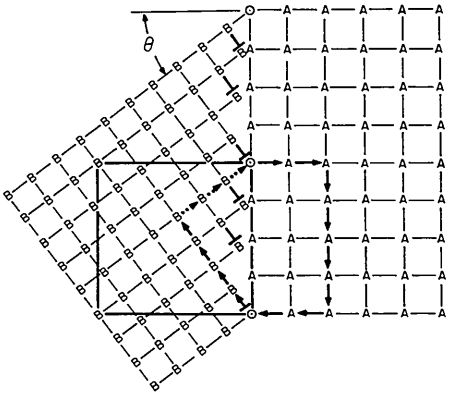

Fig. 10. A 36·9° asymmetric tilt boundary in a two-phase material.

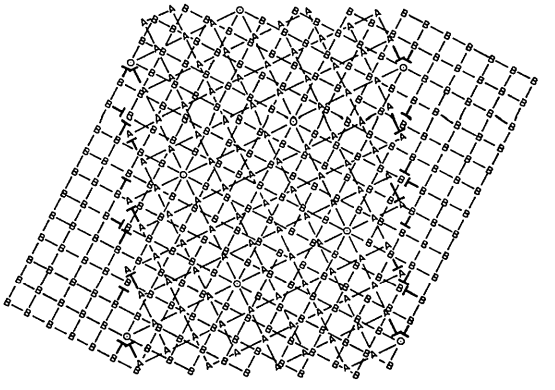

Fig. 11. A 53·1° interphase twist boundary joined to a pair of symmetric interphase tilt boundaries.

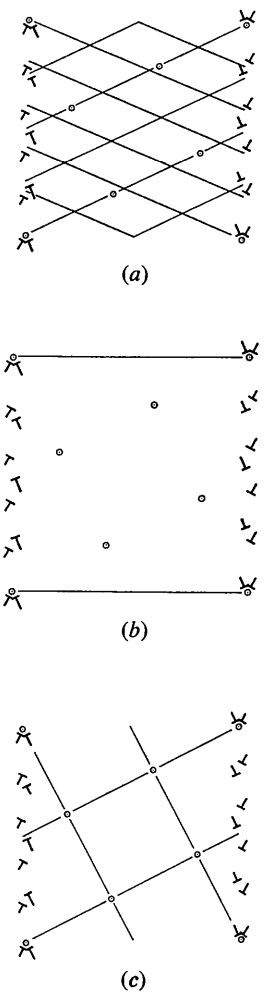

Fig. 12. (*a*) Interphase twist boundary of Fig. 11 in which only the interphase crystal-lattice dislocations are visible. (*b*) Interphase twist boundary of Fig. 11 in which a set of interphase boundary dislocations associated with the larger of two possible coincidence-site lattices is visible. (*c*) Interphase twist boundary of Fig. 11 in which a set of interphase boundary dislocations associated with the smaller of two possible coincidence-site lattices is visible.

cube axis. In general, any crystallographic axis can be employed (Marcinkowski, Tseng & Dwarakadasa, 1974*b*), but with a corresponding increase in the complexity of the analysis.

Secondly, any coincidence-site lattice can be generated from any other coincidence-site lattice in the same manner by which the coincidence-site lattices of the present analysis were described as being derived from the original crystal lattice. When using the coincidence-site-lattice unit cell as an initial reference lattice, the sublattice of the initial coincidence-site lattice is used to describe the Burgers vectors of the dislocations which carry the initial coincidence-site lattice to the final one (Marcinkowski & Sadananda, 1975).

Summary and conclusions

A coincidence-site-lattice theory of grain boundaries has been extended to include simple two-phase interfaces, *i.e.* simple cubic structures of differing lattice constant. Interphase boundaries with no tilt or twist as well as those with both symmetric and asymmetric tilt as well as pure twist have been considered. It has been shown that a characteristic coincidence-site lattice can be associated with each particular type of boundary. The Burgers circuit about an interphase boundary has also been discussed in detail in terms of both the crystal lattice and coincidence-site lattice and is shown to adequately describe the dislocation content within the boundary.

The present research effort was supported by The National Science Foundation under Grant No. GH-32262.

References

BOLLMANN, W. (1970). *Crystal Defects and Crystalline Interfaces*. New York: Springer–Verlag.

CULLEN, W. H. JR, MARCINKOWSKI, M. J. & DAS, E. S. P. (1973). *Surface Sci.* **36**, 395–413.

HIRTH, J. P. & LOTHE, J. (1968). *Theory of Dislocations*. New York: McGraw–Hill.

MARCINKOWSKI, M. J. (1970*a*). *Fundamental Aspects of Dislocation Theory*, NBS Spec. Publ. No. 317, Vol. 1, edited by J. A. SIMMONS, R. DEWIT and R. BULLOUGH, pp. 531–545.

MARCINKOWSKI, M. J. (1970*b*). *Microscopie Electronique* **1970**, Vol. I, *Proc. Seventh Int. Congress for Electron Microscopy, Grenoble* (1970). Edited by P. FAVARD, pp. 51–52. Paris: Sociéte de Microscopie Electronique.

MARCINKOWSKI, M. J. (1972). *Electron Microscopy and Structure of Materials*, Edited by G. THOMAS, R. M. FULRATH and R. M. FISHER, pp. 382–416. Berkeley: Univ. of California Press.

MARCINKOWSKI, M. J. & DWARAKADASA, E. S. (1973). *Phys. Stat. Sol.* (*a*), **19**, 597–608.

MARCINKOWSKI, M. J. & KRÖNER, E. (1975). To be published.

MARCINKOWSKI, M. J. & SADANANDA, K. (1973). *Phys. Stat. Sol.* (*a*), **18**, 361–375.

MARCINKOWSKI, M. J. & SADANANDA, K. (1975). *Acta Cryst.* A**31**, 280–292.

MARCINKOWSKI, M. J., SADANANDA, K. & TSENG, WEN FENG (1973). *Phys. Stat. Sol.* (*a*), **17**, 423–433.

MARCINKOWSKI, M. J. & TSENG, WEN FENG (1970). *Met. Trans.* **1**, 3397–3401.

MARCINKOWSKI, M. J., TSENG, WEN FENG & DWARAKADASA, E. S. (1974*a*). *Phys. Stat. Sol.* (*a*), **22**, 659–669.

MARCINKOWSKI, M. J., TSENG, WEN FENG & DWARAKADASA, E. S. (1974*b*). *J. Mater. Sci.* **9**, 29–40.

SADANANDA, K. & MARCINKOWSKI, M. J. (1974*a*). *J. Mater. Sci.* **9**, 245–257.

SADANANDA, K. & MARCINKOWSKI, M. J. (1974*b*). *J. Appl. Phys.* **45**, 1521–1532.

WEERTMAN, J. & WEERTMAN, J. R. (1964). *Elementary Dislocation Theory*. New York: Macmillan.